

# Quantitative analysis of spectral differential reflectivity in the radar bright band

A. D. Hassiotis, N. C. Skaropoulos, and H. W. J. Russchenberg

International Research Center for Telecommunications-Transmission and Radar, Delft University of Technology, Mekelweg 4, 2628CD, Delft, The Netherlands

**Abstract.** Doppler polarimetric radar observations in the radar bright band are presented and discussed. The emphasis is on the spectral differential reflectivity (i.e., the distribution of  $Z_{DR}$  in the Doppler velocity spectrum), which is a parameter that provides insight into the size-shape relationship of the melting hydrometeors. The evolution of the spectral differential reflectivity with the depth below the  $0^\circ\text{C}$  isotherm is studied in detail for a single melting layer event. A quantitative analysis demonstrates the structure of this parameter, despite the great complexity of the microphysical processes taking place.

## 1 Introduction

During stratiform precipitation, raindrops are formed from melting snowflakes. Ice needles and plates aggregate and form snowflakes, which begin to melt when they fall through the  $0^\circ\text{C}$  isotherm in the atmosphere. Just below this level, the water-coated snowflakes increase the radar reflectivity with respect to the snow region above, whereas further below, the melting snowflakes collapse into raindrops, small compared to the initial snow flakes, and their fall speed increases resulting in a net reduction of particle concentration, and hence in reduced reflectivity. This region of enhanced reflectivity is commonly known as the radar bright band. Our understanding of the microphysical changes which take place in the bright band is still far from complete. While in-situ measurements are useful in determining snowflake size distributions at discrete locations in the melting layer, they suffer from undersampling. With the advances in Doppler-polarimetric radar, an opportunity now exists to profile the melting layer on scales comparable to scales where microphysical properties may change.

In this paper we present quantitative measurements of the spectral differential reflectivity,  $sZ_{DR}$ , which is defined as

the difference in radar reflectivity factor at horizontal and vertical polarization as a function of fall velocity. Analysis of the distribution of  $sZ_{DR}$  in the Doppler velocity spectrum provides insight into the size-shape relationship of the hydrometeors (Verlinde et al., 2002). To quantify this relationship, which is needed for models of electromagnetic wave backscattering by and propagation through the melting layer, the curvature of the slope is approximated using a least-squares linear regression fit.

High resolution Doppler-polarimetric measurements were taken by the 3.3 GHz Transportable Atmospheric Radar (TARA), operated by the Technical University of Delft, during uniform, continuous rain on 19 September 2001. The measurements formed part of the BBC campaign at the Cabauw Experimental Site for Atmospheric Research (CE-SAR) in the Netherlands (CLIWANET home page).

## 2 Methodology

A 75 s period was selected for detailed analysis (Fig. 1). During this period, the  $0^\circ\text{C}$  isotherm was located at about 2000 m. The radar elevation angle was  $45^\circ$ , and the height resolution was 11 m. Main beam polarization (HH, HV, VV) was switched on a sweep-to-sweep basis (i.e., every 1 ms) with Doppler spectra, for each individual setting, being generated every 2.5 s. Power spectra were smoothed using an iterative differences filter. The spectra were then unfolded, and shifted to  $0\text{ ms}^{-1}$ , using the first moment (mean velocity) of the horizontal reflectivity spectrum. Averaging was carried out on all spectra over the 75 s period. The spectral differential reflectivity,  $sZ_{DR}$ , was finally calculated as the ratio of the mean horizontal and vertical reflectivity factors,  $Z_{hh}$  and  $Z_{vv}$ , per velocity bin:

$$sZ_{DR}(\nu) = 10 \log \frac{Z_{hh}(\nu)}{Z_{vv}(\nu)}. \quad (1)$$

Spectrographs of  $Z_{hh}$  and  $Z_{DR}$  can be seen in Fig. 2. The convention used in this paper is that negative velocities are

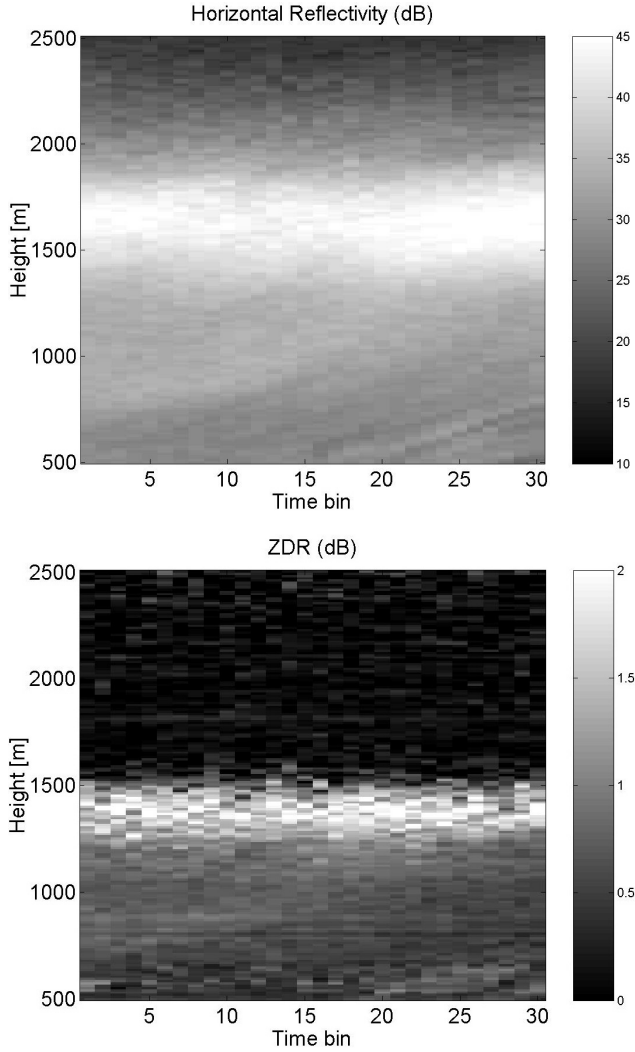


**Fig. 1.** Time-height sections of  $Z_{hh}$  and  $Z_{DR}$  for the 75 s analysis interval.

approaching the radar. Thus, hydrometeors falling with velocities larger than the mean velocity appear on the left side of the Doppler spectra, whereas slower-falling hydrometeors appear on the right side. Noticeable in the  $sZ_{DR}$  panel, is a reversal in slope with melting. In the upper layer, this slope is positive with high values of  $sZ_{DR}$  at the right edges of the spectra and lower values at the left edges. This may be due to the presence of slow-falling, horizontally-aligned, pristine ice crystals and plates at the right edges of the spectra, and faster-falling, loose aggregates of snow crystals with decreasing  $sZ_{DR}$  in the middle to left edges of the spectra (Verlinde et al., 2002). As the snow aggregates turn into rain, the  $sZ_{DR}$  slope reverses becoming negative, with high values of  $sZ_{DR}$  now at the left edges of the spectra and lower values at the right edges. This is the result of large, faster-falling, oblate raindrops at the left edges of the spectra, and smaller, slower-falling, spherical raindrops at the right edges of the spectra. A detailed view of the evolution of this slope change in the bright band will be presented in the next section. Figure 3

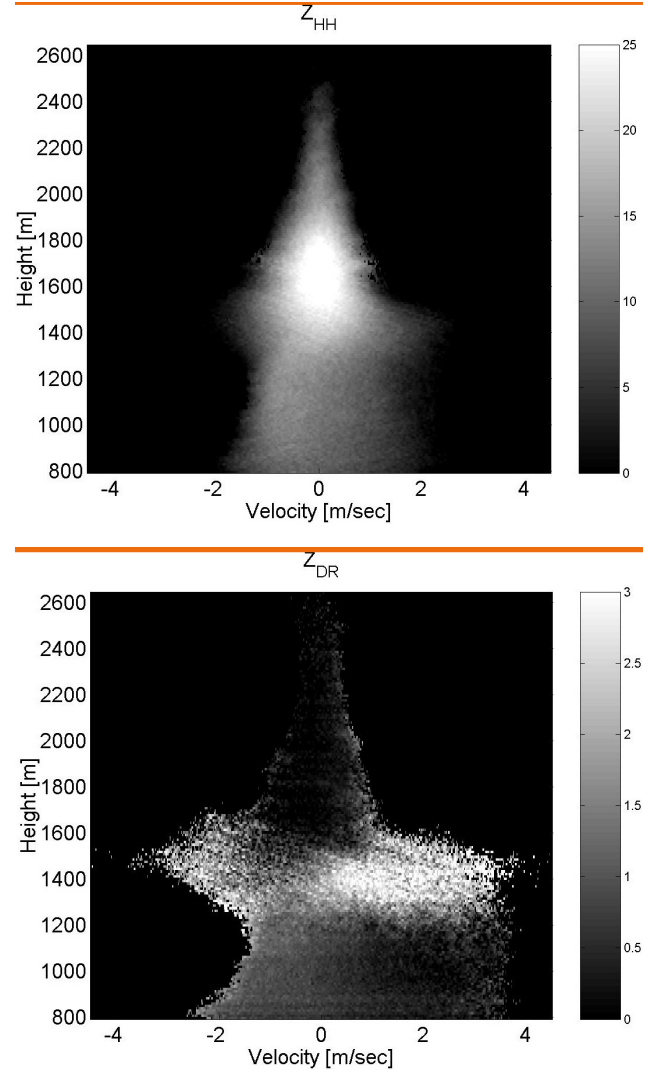


**Fig. 2.** Spectrographs of  $Z_{hh}$  and  $Z_{DR}$ .

shows the height profiles of  $Z_{hh}$ ,  $Z_{DR}$ , and the linear depolarization ratio,  $L_{DR}$ . The dashed lines indicate the three characteristic features of the bright band: the top, the bottom and the peak of the bright band. The thickness of the bright band is extracted, in a somewhat arbitrary manner, by visual inspection of the  $Z_{hh}$  reflectivity profile and of the  $Z_{hh}$  spectrograph. The bright band can be parameterized using a position parameter  $H$  (Barthazy, 1998). At the top of the bright band  $H$  is set to 1, at the peak value  $H$  is 0, and at the bottom of the bright band  $H$  is  $-1$ . The use of positive and negative values for  $H$  accounts for the fact that the  $Z_{hh}$  profile is not symmetric. An important advantage of the parameterization is that it allows measurements with differing bright band characteristics to be compared.

### 3 Results and discussion

Fig. 4 and Fig. 5 shows each individual  $Z_{DR}$  spectrum in the upper and lower bright band, respectively. The width of

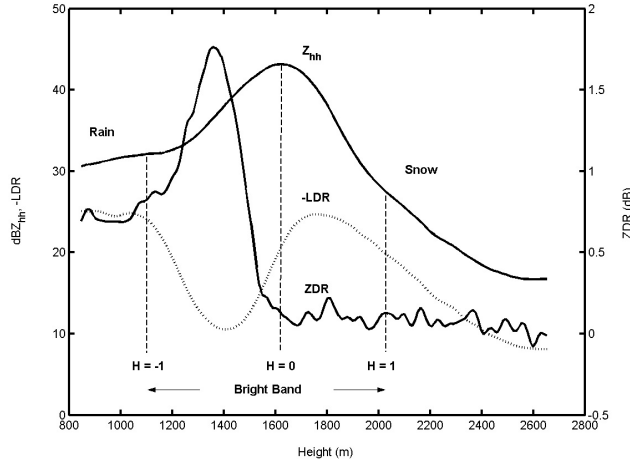


**Fig. 3.** Radar reflectivity profiles of the bright band. The three vertical lines indicate the thickness and peak of the bright band. The bright band has been parameterised using position parameter,  $H$ .

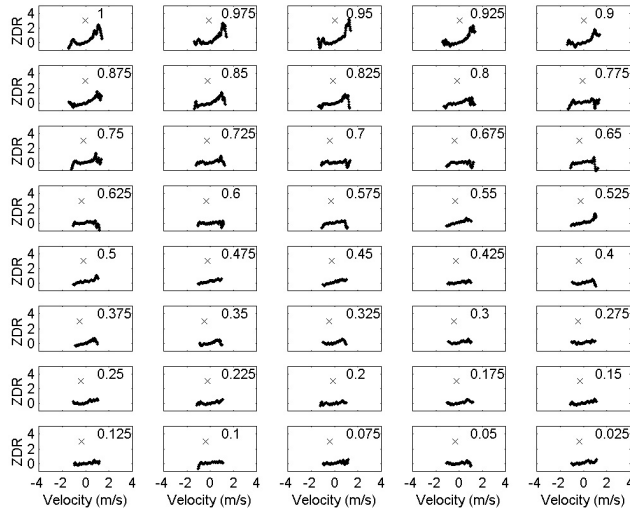


**Fig. 4.** Spectral evolution of  $Z_{DR}$  in the upper bright band in dependence of position parameter,  $H$  (top, right corner of each panel). The “plus” symbol denotes the value of the skewness coefficient.

each spectrum is related to the variance (second moment) of  $sZ_{hh}$ . The asymmetry of  $sZ_{hh}$  is measured by the skewness coefficient (third moment). Its value is given by the relative location of the “x” symbol on the horizontal axis. A positive value denotes a tail at the right edge, a negative value a tail at the left edge. In the upper right corner is the value of  $H$ , which indicates the spectrum’s position in the bright band.

Melting begins at a height of about 2050 m ( $H = 1$ ). The slope of  $sZ_{DR}$  is approximately  $0.5 \text{ dB/ms}^{-1}$ . A shoulder of magnitude 3 dB is observed at the right edge of the  $sZ_{DR}$  spectrum. Power spectra are narrow ( $0.35 \text{ ms}^{-1}$ ) and symmetric, and the overall reflectivity is low. These observations would be consistent with a radar volume consisting of snow crystals and aggregates (Verlinde et al., 2002). Slow-falling,

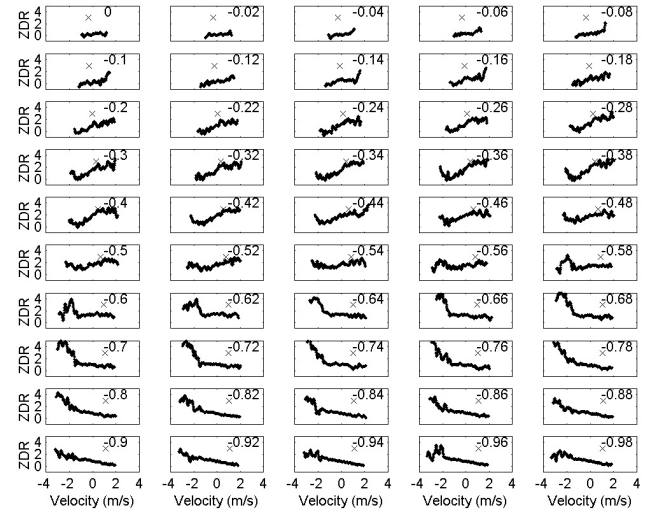


**Fig. 5.** Same as Fig. 4, but in the lower bright band.

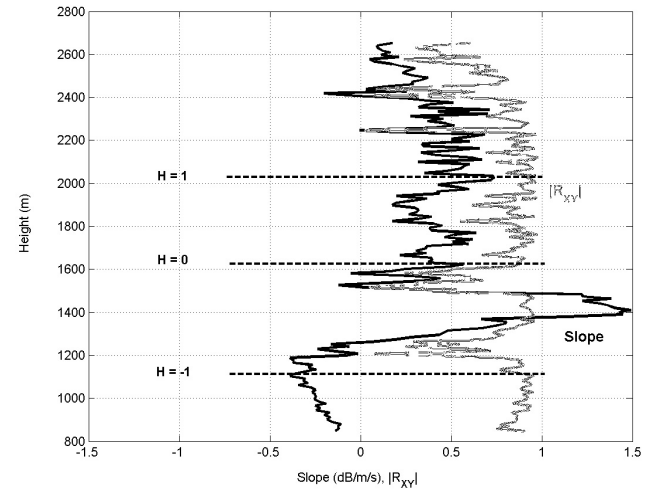


**Fig. 6.** Height profile of the estimated  $sZ_{DR}$  slope (black curve), and the validity of the linear fit (grey curve).

horizontally-aligned, pristine ice crystals and plates to the right of the spectrum give a non-zero  $Z_{DR}$ . Faster falling, loose aggregates of snow crystals with decreasing density, and thus lower  $Z_{DR}$  (due to a reduction in effective permittivity), comprise the middle to left edge of the spectrum, resulting in a positive  $sZ_{DR}$  slope. In the region between  $H = 1$  and  $H = 0.775$ , the shoulder at the right edge drops to a value of 1.5 dB, and the slope of  $sZ_{DR}$  decreases to around  $0.3 \text{ dB/ms}^{-1}$ . This drop suggests that many of the slow-falling snow crystals have in the space of 100 m already melted into small, spherical raindrops, thus causing the right shoulder of  $sZ_{DR}$  to disappear.

Deeper into the upper bright band, the slope increases steadily to a value of about  $0.6 \text{ dB/ms}^{-1}$  at  $H = 0.375$ . The skewness coefficient is about  $-0.5 \text{ ms}^{-1}$  as the power spectrum is now skewed to the right. This could indicate a region of increased aggregation in which “stickier”, wetted aggre-

gates have a higher probability of accumulating more snow crystals. Between  $H = 0.375$  and  $H = -0.08$ , the  $sZ_{DR}$  slope flattens. Due to a high variability in this region, the linear approximation is questionable. An increase in depolarisation is observed as the  $L_{DR}$  profile begins to become measurable. These observations could be attributed to the irregular, rotating and oscillating motions experienced by large snowflakes, when they start melting, as it has been reported in laboratory observations (Mitra et al., 1990).

As melting continues, the right edge of  $sZ_{DR}$  begins to increase dramatically. The power spectrum broadens, developing a tail at the left edge. A maximum slope of  $1.5 \text{ dB/ms}^{-1}$  is observed around  $H = -0.4$ . The increased permittivity of melting, less-compact aggregates may account for this steep slope. At the same time, the spectrum begins flaring out. This larger particle fall-velocity distribution may be due to an increasing population of raindrops. Below  $H = -0.4$ , the slope begins to fall rapidly, becoming negative around  $H = -0.7$ . The power spectrum exhibits an increasingly long tail on the right side. A shoulder at the left edge of  $sZ_{DR}$  rises to about 4 dB ( $H = -0.66$ ). These rapid changes are probably due to the compaction of the aggregates into large, oblate raindrops. After compaction, the particles accelerate appearing at the left edge of the spectrum. The right edge of the spectrum is now inhabited solely by the slower-falling, spherical droplets. Noticeably, the shoulder at the left edge begins to drop rapidly below  $H = -0.78$ . It has been speculated that this may be due to breakup (Verlinde et al., 2002). At the bottom of the bright band ( $H = -1$ ) the slope is highly linear and negative. The hydrometeor population consists solely of rain.

In Fig. 6, the results of the linear regression fitting are shown. The fitted slope (black curve) and the validity of the linear fit,  $R_{XY}$ , (grey curve) are plotted as a function of height. Curve fitting was applied to  $sZ_{DR}$  one spectrum width either side of  $0 \text{ ms}^{-1}$ . This selection windowed the core of the spectrum, thus avoiding the edge effects. In the figure, the absolute value of  $R_{XY}$  is well above 0.5 through

most of the bright band, suggesting that in those parts a linear approximation is valid. Just below the peak of the bright band, however, the fitting is degraded by a high variability in  $sZ_{DR}$ , possibly due to the wild, helical motions of the “dry” aggregates.

#### 4 Conclusion

The spectral differential reflectivity,  $sZ_{DR}$ , is a radar observable that provides insight into the size-shape relationship of precipitating hydrometeors. For the first time its evolution through the bright band has been quantified using linear regression fitting. The linear approximation holds through most of the bright band, revealing size-shape trends of the hydrometeors despite the great complexity of the microphysical changes taking place. The results of this study can be useful to models of electromagnetic wave scattering by and propagation through the melting layer of precipitation. Yet, many more Doppler-polarimetric measurements are required to validate and interpret the trends of  $sZ_{DR}$  reported herein. Future work will involve incorporating spectral data into a radar-derived microphysical model.

#### References

- Barthazy E.J., Microphysical properties of the melting layer, PhD dissertation, Swiss Federate Institute of Technology, Diss. ETH No. 12687, 1998.
- CLIWA-NET: Home page of the cloud liquid water content network, <http://www.knmi.nl/samenw/cliwa-net/index.html>.
- Mitra, S.K., Vohl, O., Ahr, M., and Pruppacher, H.R.: A wind tunnel and theoretical study of the melting behaviour of atmospheric ice particles. Part IV: Experiment and theory for snow flakes, *J. Atmos. Sci.*, 47, 584-591, 1990.
- Verlinde, J., Moiseev, D., Skaropoulos, N.C., Hassiotis, A., Heijnen, S.H., V.d. Zwan, W.F., and Russchenberg, H.W.J.: Spectral polarimetric measurements in the radar bright band, submitted for publication to *Journal of Atmospheric and Oceanic Technology*, 2002.